

High quality InAlN single layers lattice-matched to GaN grown by molecular beam epitaxy

Ž. Gačević,^{1,a)} S. Fernández-Garrido,^{1,b)} J. M. Rebled,^{2,c)} S. Estradé,^{2,3} F. Peiró,² and E. Calleja¹

¹ISOM, Universidad Politécnica de Madrid, Avda. Complutense s/n, 28040 Madrid, Spain

²LENS-MIND-IN2UB, Departament d'Electrònica, Universitat de Barcelona, Martí i Franquès 1, 08028 Barcelona, Spain

³TEM-MAT, CCiT-UB, Solé i Sabarís 1, 08028 Barcelona, Spain

We report on properties of high quality ~ 60 nm thick InAlN layers nearly in-plane lattice-matched to GaN, grown on *c*-plane GaN-on-sapphire templates by plasma-assisted molecular beam epitaxy. Excellent crystalline quality and low surface roughness are confirmed by X-ray diffraction, transmission electron microscopy, and atomic force microscopy. High annular dark field observations reveal a periodic in-plane indium content variation (8 nm period), whereas optical measurements evidence certain residual absorption below the band-gap. The indium fluctuation is estimated to be $\pm 1.2\%$ around the nominal 17% indium content via plasmon energy oscillations assessed by electron energy loss spectroscopy with sub-nanometric spatial resolution.

The III-nitrides combine unique properties, such as direct band gap, tuneable from near infra-red (0.7 eV, InN) to near ultra-violet (6.2 eV, AlN) range, with high excitonic binding energy. This makes them attractive materials for research and perfect candidates for high efficiency light emitters.¹ Their huge potential, however, has been significantly constrained by the high *in-plane* lattice mismatch between the three binaries (InN, GaN, and AlN) that inevitably leads to defect formation at heterostructures' interfaces, affecting detrimentally their (opto)electronic properties. The InAlN ternary compound, with approximately 17% of indium, grows *in-plane* lattice-matched (LM) to GaN, offering thus potential for strain-free heterostructures that could revolutionize several fields, such as high electron mobility transistors (HEMTs), near infra-red devices based on intersubband transitions as well as resonant cavity based optoelectronic devices. Due to high miscibility gap between InN and AlN binaries, early theoretical calculations based on strictly regular solution model predicted high mixing instability and strong spinodal decomposition of InAlN material.² Despite the expectations, high quality InAlN based devices, grown mainly by metal organic vapor phase epitaxy (MOVPE), have been demonstrated.^{3–6} Reports concerning molecular beam epitaxy (MBE) growth are very scarce and have been mainly focused on HEMTs.^{7–14}

Difficulties to fabricate high quality LM InAlN/GaN heterostructures concern the following issues: high crystalline quality and good homogeneity of InAlN layers as well as flat and abrupt heterostructure interfaces. In general, MBE growth technique facilitates the formation of exceptionally flat and abrupt interfaces and, thus, offers potential for

further improvements. In this work, we give valuable insight into properties of high quality InAlN layers grown by MBE, relevant for the fabrication of LM InAlN/GaN distributed Bragg reflectors (DBRs) and other devices based on strain-free heterostructures.

The samples under study were grown in a RIBER Compact 21 MBE system equipped with a radio-frequency plasma nitrogen source and standard Knudsen cells for Ga, Al, and In. Approximately 4 μm thick GaN templates, grown on *c*-plane sapphire by MOVPE were used as substrates. Previous to InAlN growth, a ~ 100 nm thick GaN buffer layer was grown under intermediate Ga-rich conditions to bury possible impurities and to provide a flat surface.¹⁵ InAlN layers were grown at 535 °C on the boundary between In-droplets and N-rich growth regimes (i.e., under effective III-N stoichiometry), yielding layers free of droplets with typically $17\% \pm 2\%$ indium content.^{12,14} Growth times were set to 20 ± 2 min, which resulted in layers 50-60 nm thick. Let us note that these values correspond to the thickness of one InAlN semi-period, inserted into a DBR targeted for blue/green applications, respectively.^{13,14}

The crystal quality of the samples was assessed by X-ray diffraction (XRD) scans and reciprocal space maps around the [0002] and [10 $\bar{1}$ 5] Bragg reflections using an X'Pert PRO PANalytical diffractometer. Figure 1(a) shows the $\omega/2\theta$ and ω -rocking scans around [0002] Bragg reflection of a 58 nm thick $\text{In}_{0.17}\text{Al}_{0.83}\text{N}$ layer. Only peaks corresponding to the InAlN epilayer, GaN template, and sapphire (omitted here for clarity) are observed, showing thus no trace of InN-AlN phase separation. The full width at half maximum (FWHM) of the ω -rocking curves of the InAlN epilayers and the GaN templates are found to be equal $\sim 0.1^\circ/0.1^\circ$, around both the symmetric [0002] and the asymmetric [10 $\bar{1}$ 5] reflections, suggesting that the crystal quality of the InAlN layer may be limited by that of the underneath GaN template. In addition, the same value of 0.1° around the symmetric [0002] reflection has been reported for ~ 500 nm thick

^{a)} Author to whom correspondence should be addressed. Electronic mail: gacevic@isom.upm.es.

^{b)} Present address: Paul-Drude-Institut für Solid State Electronics, Hausvogteiplatz 5-7, 10117 Berlin, Germany.

^{c)} Also at Institute of Materials Science (ICMAB-CSIC), Campus UAB, 08193 Bellaterra, Spain.

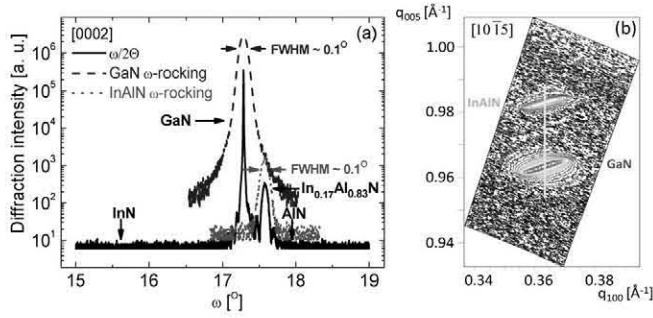


FIG. 1. (Color online) (a) $\omega/2\theta$ and ω -rocking scans around [0002] Bragg spot of a single In_{0.17}Al_{0.83}N layer. The scans are characterized by no trace of phase separation and good FWHM of InAlN ω -rocking curves. (b) RSM of a single In_{0.15}Al_{0.85}N layer around [1015] Bragg spot confirms *in-plane* lattice accommodation to the underneath GaN pseudo-substrate.

MOVPE InAlN layers grown on a GaN template.¹⁶ Reciprocal space mapping (RSM) around the asymmetric [1015] reflection (Figure 1(b)) confirms that all the samples (with $17\% \pm 2\%$ indium content) have grown with the *in-plane* lattice constant accommodated to the underneath GaN substrate. The *in-plane* strain in the accommodated layers is found to be within $\pm 4 \times 10^{-3}$ range, as estimated by the linear III-nitride elasticity theory.

Figure 2 (left) features typical InAlN surface morphology, as measured by tapping-mode Digital Instruments MMAFM-2 atomic force microscopy (AFM). Flat surface with atomic steps is observed, with root mean square (RMS) surface roughness of ~ 0.6 nm, over $2.5 \times 2.5 \mu\text{m}^2$ scan area. This value is only slightly higher than the typical ~ 0.4 nm RMS roughness of the underneath GaN template and similar to ~ 0.7 nm value, reported for ~ 100 nm thick InAlN layers grown by MOVPE.¹⁶

High-resolution transmission electron microscopy (HRTEM) examinations, performed in a JEOL J2010F (S)TEM operating at 200 keV and coupled with a Gatan Imaging Filter spectrometer, confirmed that InAlN crystallizes in hexagonal wurtzite phase (Fig. 3(a)). No cubic inclusions were observed. In addition, no crystallographic defects formation was found in the layer. The fast Fourier transformation (FFT) of the HRTEM image of the InAlN/GaN interface (Fig. 3(b)) confirms that InAlN layer grows *in-plane* accommodated to the GaN substrate, with the expected epitaxial relationship (0001)[11-20]InAlN||[0001][11-20]GaN. High angle annular dark field (HAADF) observations (Fig. 3(c)) revealed periodic contrast modulations with ~ 8 nm period. This contrast modulation is attributed to indium content fluctuation that originates from spinodal decomposition of the material. To further inves-

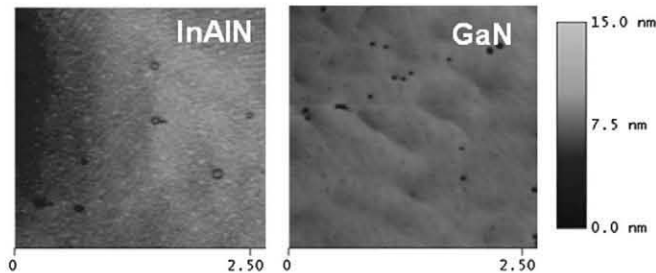


FIG. 2. (Color online) $2.5 \times 2.5 \mu\text{m}^2$ AFM images of the typical InAlN (left) and GaN (right) surface morphology.

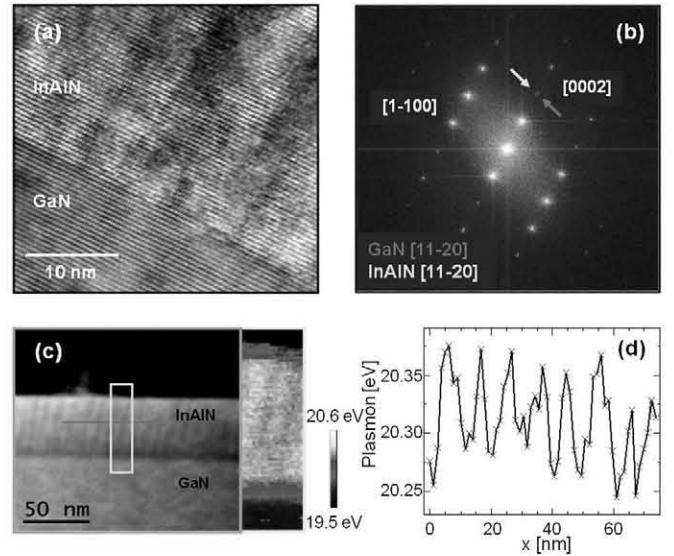


FIG. 3. (Color online) HRTEM image (a) and the corresponding FFT power spectrum (b) of the InAlN/GaN interface confirm excellent crystalline quality and perfect lattice-matching of the InAlN to the underneath GaN. HAADF image (c) reveals indium content fluctuations further confirmed by high-resolution EELS studies (d) of InAlN Plasmon peak energy.

tigate this point, the samples were characterized by electron energy loss spectroscopy (EELS). This technique allows for Plasmon energy monitoring with exceptionally high spatial resolution (Fig. 3(d)). The Plasmon peak energy is found to oscillate around 20.32 eV, with ~ 0.12 eV peak-to-valley amplitude. Bearing in mind that InN and AlN plasmon energies are 15.7 and 21.1 eV, respectively,^{17,18} the indium content fluctuation can be roughly estimated within linear Vegard law approximation: $dE_p(\text{In}_x\text{Al}_{1-x}\text{N})/dx = E_p(\text{InN}) - E_p(\text{AlN})$, yielding $\pm 1.2\%$ value.

Let us recall that the InAlN/GaN combination exhibits relatively low refractive index contrast ($\sim 7.2\%$)¹⁶ that in the case of DBRs provokes significant penetration depth of the incident light into the structure, making it very sensitive to the presence of residual absorption which is detrimental for reflectivity.¹⁴ To gain some insight into optical properties, the samples have been characterized by a JASCO V-650 spectrophotometer. The residual absorption (A) was assessed indirectly, via reflectivity (R) and transmittivity (T) measurements, ($A(\lambda) = 1 - R(\lambda) - T(\lambda)$), performed at nearly normal incidence. Fig. 4 features absorption of a ~ 60 nm thick In_{0.17}Al_{0.83}N on GaN template and a reference GaN template. The onset of GaN band gap absorption around 3.4 eV screens the onset of InAlN band gap absorption, since it is expected at much higher energies (> 4 eV).¹⁶ However, residual absorption, as high as 2% and 5% in the green and blue spectral regions, respectively, is confirmed and attributed to InAlN epilayer. Bearing in mind the excellent crystalline quality (confirmed by XRD and TEM techniques) as well as absence of regions with exceptionally high In content (confirmed by EELS measurements), this result is somewhat surprising and we link it to incident photon scattering on InAlN inhomogeneities. In spectrophotometric measurements, InAlN/GaN bi-layer is sandwiched between air and sapphire. We speculate that incident photons scattered on InAlN inhomogeneities at low angle with respect to the

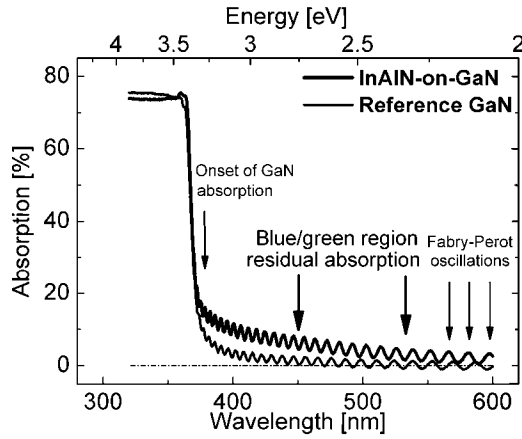


FIG. 4. (Color online) Absorption measurements of a ~ 60 nm thick $\text{In}_{0.17}\text{Al}_{0.83}\text{N}$ on GaN template. Absorption of reference GaN template is also featured for comparison.

interfaces remain captured inside the InAlN/GaN bi-layer due to total reflection on high refractive index contrast interfaces: InAlN/air ($\sim 2.32/1.0$) and GaN/sapphire ($\sim 2.5/1.78$), until they are absorbed by defects in the material.

In summary, we demonstrate the MBE growth of flat InAlN layers LM to GaN with exceptionally high crystalline quality. The fluctuation in indium content, attributed to spinodal decomposition, is estimated to be within the $17.0\% \pm 1.2\%$ range and has been linked to the presence of residual absorption in the green/blue spectral range. We point out that surface roughness, defect formation, and overall crystalline quality of MBE grown InAlN layers seem to be mastered. However, according to our evidence, their high homogeneity still remains a challenge, being thus the last obstacle to surmount before their exploitations in MBE grown III-nitride devices.

This work was partially supported by research grants from the Spanish Ministry of Education under Grant Nos.

MAT2008-04815, MAT2010-16407, Consolider CSD2006-19, and Consolider CSD2009-00013 and the Community of Madrid under Grant No. P2009/ESP-1503. We also acknowledge technical support from Scientific and Technical Center (CCiT) of the University of Barcelona.

- ¹S. Nakamura and G. Fasol, *The Blue Laser Diode* (Springer, Berlin, 1997).
- ²T. Matsuoka, Appl. Phys. Lett. **71**, 105 (1997).
- ³J. F. Carlin and M. Ilegems, Appl. Phys. Lett. **83**, 668 (2003).
- ⁴J. Dorsaz, J.-F. Carlin, C. M. Zellweger, S. Gradecak, and M. Ilegems, Phys. Status Solidi **201**, 2675 (2004).
- ⁵E. Feltn, R. Butte, J. F. Carlin, J. Dorsaz, N. Grandjean, and M. Ilegems, Electron. Lett. **41**, 94 (2005).
- ⁶E. Feltn, G. Christmann, J. Dorsaz, A. Castiglia, J. F. Carlin, R. Butte, N. Grandjean, S. Christopoulos, G. B. H. von Hogerthal, A. J. D. Grundy, P. G. Lagoudakis, and J. J. Baumberg, Electron. Lett. **43**, 924 (2007).
- ⁷D. S. Katzer, D. F. Storm, S. C. Binari, B. V. Shanabrook, A. Torabi, L. Zhou, and D. J. Smith, J. Vac. Sci. Technol. B **23**, 1204 (2005).
- ⁸K. Jeganathan, M. Shimizu, H. Okumura, Y. Yano, and N. Akutsu, J. Cryst. Growth **304**, 342 (2007).
- ⁹S. Dasgupta, Nidhi, S. Choi, F. Wu, J. S. Speck, and U. Mishra, Appl. Phys. Express **4**, 045502 (2011).
- ¹⁰S. Schmult, T. Siegrist, A. M. Sergent, M. J. Manfra, and R. J. Molnar, Appl. Phys. Lett. **90**, 021922 (2007).
- ¹¹T. Ive, O. Brandt, X. Kong, A. Trampert, and K. H. Ploog, Phys. Rev. B **78**, 035311(2008).
- ¹²S. Fernández-Garrido, Ž. Gačević, and E. Calleja, Appl. Phys. Lett. **93**, 161907 (2008).
- ¹³Ž. Gačević, S. Fernández-Garrido, E. Calleja, E. Luna, and A. Trampert, Phys. Status Solidi C **6**, S643 (2009).
- ¹⁴Ž. Gačević, S. Fernández-Garrido, D. Hosseini, S. Estradé, F. Peiró, and E. Calleja, J. Appl. Phys. **108**, 113117 (2010).
- ¹⁵G. Koblmüller, S. Fernandez-Garrido, E. Calleja, and J. S. Speck, Appl. Phys. Lett. **91**, 161904 (2007).
- ¹⁶R. Butté, J. F. Carlin, E. Feltn, M. Gonschorek, S. Nicolay, G. Christmann, D. Simeonov, A. Castiglia, J. Dorsaz, H. J. Buehlmann, S. Christopoulos, G. B. H. von Högerthal, A. J. D. Grundy, M. Mosca, C. Pinquier, M. A. Py, F. Demangeot, J. Frandon, P. G. Lagoudakis, J. J. Baumberg, and N. Grandjean, J. Phys. D: Appl. Phys. **40**, 6328 (2007).
- ¹⁷P. Specht, J. C. Ho, X. Xu, R. Armitage, E. R. Weber, E. Erni, and C. Kisielowski, J. Cryst. Growth **288**, 225 (2006).
- ¹⁸J. C. Sánchez-López, L. Contreras, A. Fernández, A. R. González-Elipe, J. M. Martín, and B. Vacher, Thin Solid Films **317**, 100 (1998).